# Insulin signaling regulates a functional interaction between adenomatous polyposis coli and cytoplasmic dynein

Feng J. Gao[a,†], Liang Shi[b,†], Timothy Hines[b], Sachin Hebbar[c], Kristi L. Neufeld[d], and Deanna S. Smith[b,*]

[a]Department of Physiology, Johns Hopkins University School of Medicine, Baltimore, MD 21025; [b]Department of Biological Sciences, University of South Carolina, Columbia, SC 29208; [c]Department of Anesthesiology and Critical Medicine, Johns Hopkins University School of Medicine, Baltimore, MD 21287; [d]Department of Molecular Biosciences, University of Kansas, Lawrence, KS 66045

**ABSTRACT** **Diabetes is linked to an increased risk for colorectal cancer, but the mechanistic underpinnings of this clinically important effect are unclear. Here we describe an interaction between the microtubule motor cytoplasmic dynein, the adenomatous polyposis coli tumor suppressor protein (APC), and glycogen synthase kinase-3β (GSK-3β), which could shed light on this issue. GSK-3β is perhaps best known for glycogen regulation, being inhibited downstream in an insulin-signaling pathway. However, the kinase is also important in many other processes. Mutations in APC that disrupt the regulation of β-catenin by GSK-3β cause colorectal cancer in humans. Of interest, both APC and GSK-3β interact with microtubules and cellular membranes. We recently demonstrated that dynein is a GSK-3β substrate and that inhibition of GSK-3β promotes dynein-dependent transport. We now report that dynein stimulation in intestinal cells in response to acute insulin exposure (or GSK-3β inhibition) is blocked by tumor-promoting isoforms of APC that reduce an interaction between wild-type APC and dynein. We propose that under normal conditions, insulin decreases dynein binding to APC to stimulate minus end–directed transport, which could modulate endocytic and secretory systems in intestinal cells. Mutations in APC likely impair the ability to respond appropriately to insulin signaling. This is exciting because it has the potential to be a contributing factor in the development of colorectal cancer in patients with diabetes.**

**Monitoring Editor**
Erika Holzbaur
University of Pennsylvania

Received: Jul 28, 2016
Revised: Dec 23, 2016
Accepted: Dec 30, 2016

## INTRODUCTION

Diabetes has become a worldwide epidemic, and the multisystem effects of insulin insensitivity in patients with metabolic disorders contribute to an increased risk for neurological diseases and cancer (Larsson *et al.*, 2005; Yuhara *et al.*, 2011; Sasazuki *et al.*, 2013; Guraya, 2015; Ramjeesingh *et al.*, 2016). Thus, identifying potential mechanisms that could affect disease development in diabetics is an important goal. Although some estimates place the increased risk of colorectal cancer among diabetics at >50%, it is not at all clear which aspect of diabetes increases cancer risk—the disease itself (insulin resistance), the consequences of the disease (e.g., hyperglycemia), or the therapy. In fact, drugs used to treat diabetes are being considered for repurposing as chemopreventive or chemotherapeutic treatments, but the results of these studies have been confusing and sometimes contradictory (Gupta and Dubois, 2002; Chang *et al.*, 2012; Malek *et al.*, 2013; Park, 2013; Yin *et al.*, 2014; Mendonca *et al.*, 2015; Zhou *et al.*, 2015; He *et al.*, 2016; Ramjeesingh *et al.*, 2016). For example, peroxisome proliferator antigen receptor γ (PPARγ) agonists were protective against carcinogen-induced colon tumors in rats but enhanced intestinal adenoma formation in the adenomatous polyposis coli$^{+/min}$ (APC$^{+/min}$) mouse,

This article was published online ahead of print in MBoC in Press (http://www.molbiolcell.org/cgi/doi/10.1091/mbc.E16-07-0555) on January 5, 2017.

†These authors contributed equally.

*Address correspondence to: Deanna S. Smith (deannasm@biol.sc.edu).

Abbreviations used: AKT, protein kinase B; AMER, APC membrane recruitment protein; APC, adenomatous polyposis coli; cAPC, 272–amino acid C-terminal fragment of APC; DIC, dynein intermediate chain; GSK-3β, glycogen synthase kinase-3β; MIN, multiple intestinal neoplasia; nAPC, 746–amino acid N-terminal fragment of APC; PPARγ, peroxisome proliferator antigen receptor γ.

a model for familial adenomatous polyposis (Moser *et al.*, 1990, 1992; Lefebvre *et al.*, 1998; Osawa *et al.*, 2003; Marin *et al.*, 2006; Frohlich and Wahl, 2015).

Our recent finding that the insulin pathway can directly stimulate dynein-dependent trafficking may provide insight into the link between colon cancer and diabetes. We observed a change in dynein distribution in a mouse colon cell line and in a human colon cancer cell line exposed to the diabetes drug rosiglitazone. Both cell types have a radial microtubule (MT) array, with minus ends focused at the centrosome and plus ends growing toward, or anchored at, the cell periphery. In both cell types, dynein accumulated at centrosomes after exposure to rosiglitazone (Gao *et al.*, 2015). Because dynein motors translocate toward MT minus ends, this type of accumulation could occur due to increased motility or retention at minus ends. Live-cell imaging showed that the minus end–directed transport of lysosomes also increased in response to the drug, so in the case of rosiglitazone, increased dynein-based motility was likely to be involved (Gao *et al.*, 2015). Indirect effects caused by alterations in MT behavior could also contribute to changes in dynein distribution, but MTs were in general similar in treated and untreated cells.

Rosiglitazone-induced metabolic changes are believed to involve its actions as a PPARγ agonist (Tontonoz and Spiegelman, 2008; Choi *et al.*, 2014). One such physiological change is increased insulin sensitivity, but the exact mechanism by which this occurs is not well understood and may be different, depending on the cell type. A rapid molecular event triggered by insulin signaling is inactivation of glycogen synthase kinase-3β (GSK-3β) through an inhibitory phosphorylation of serine 9 (S9) by another kinase, protein kinase B (AKT; Beurel *et al.*, 2015). Rosiglitazone-induced dynein accumulation required insulin in the medium and was mimicked by GSK-3β inhibitors and blocked by AKT inhibitors, strongly suggesting that the dynein effect was due to the insulin-sensitizing function of the drug ultimately acting through GSK-3β. The mechanism for increased dynein motility may involve direct phosphorylation of dynein subunits by GSK-3β, as we identified two GSK-3β–targeted residues in two dynein intermediate chains (1B and 2C) that, when mutated, altered the binding of Ndel1, a dynein regulatory protein (Gao *et al.*, 2015).

If insulin regulates dynein, then aberrant insulin levels, often found in metabolic syndromes, could potentially affect important cellular processes controlled by dynein, such as organelle trafficking, endocytosis and secretion, and cortical MT capture (Hunt and Stephens, 2011; Hendricks *et al.*, 2012; Hancock, 2014). This in turn could promote or prevent tumorigenic changes. In the present study, we asked whether acute insulin exposure would also cause dynein to accumulate at centrosomes and indeed found this to be the case. We then asked whether cancer-causing mutations in APC could affect the dynein response to insulin signaling. Several pieces of information provided the motivation for this latter question. First, APC mutations cause colorectal cancer in humans and have been linked to changes in efficacy of diabetes drugs as chemotherapeutics (Lefebvre *et al.*, 1998; Gupta and Dubois, 2002; Niho *et al.*, 2003; Friedrich *et al.*, 2013). Second, APC binds and regulates MTs, which are the tracks for dynein cargo transport (Barth *et al.*, 2002, 2008; Mogensen *et al.*, 2002; Reilein and Nelson, 2005; Bahmanyar *et al.*, 2009). Third, the APC-interacting protein EB1 binds directly to dynactin, a dynein-interacting protein (Berrueta *et al.*, 1999; Ligon *et al.*, 2006; Yan *et al.*, 2015). Finally, APC and GSK-3β have been implicated in some of the same cellular processes as dynein (Dujardin and Vallee, 2002; Wen *et al.*, 2004; Hanson and Miller, 2005; Etienne-Manneville, 2009; Fleming *et al.*, 2009; Radulescu *et al.*, 2010; Beurel *et al.*, 2015). In the course of these studies, we identified a novel physical and functional link between APC and dynein and provide evidence that this interaction is sensitive to GSK-3β activity. We also show that tumor-promoting APC mutations affect the interaction. Our findings will be important for the development, screening, and testing of potential chemotherapeutics related to insulin and diabetes drugs. In addition, they may provide explanations for conflicting results and unexpected side effects of drug treatments.

## RESULTS

### Tumor-promoting APC isoforms alter the dynein response to acute insulin exposure

We used two cell lines derived from mouse colon for these experiments. One cell line was derived from the $APC^{+/min}$ mouse, which carries a mutation in one APC allele resulting in expression of a truncated APC isoform (Whitehead *et al.*, 1993; Whitehead and Joseph, 1994). The mutant cell line will be referred to here as multiple intestinal neoplasia (MIN) cells. A colon cell line derived from wild-type mice (WT cells) was used as a control for the mutation (Whitehead *et al.*, 1993; Whitehead and Joseph, 1994). We confirmed that only the MIN cells carry the mutant "MIN" isoform, using genotyping primers (Figure 1A). We also used PCR to amplify the region of the APC gene that carries the T-A point mutation in the MIN allele. In extracts derived from WT cells, only the WT sequence was present, but in the MIN cells, both WT and mutant sequences were present. This shows that the MIN genome retains a copy of the WT allele (unpublished data). Next we determined that a 1-h exposure to insulin produced the same degree of GSK-3β inhibition in MIN and WT cells. This was accomplished by comparing the ratio of the inhibited phospho-S9 GSK-3β isoforms to total GSK-3β (Figure 1, B–D). The S9 phosphorylation returned to baseline by 6 h in both cell types, likely due to insulin receptor internalization and abrogated signaling (Saltiel and Pessin, 2002). Dynein accumulation at centrosomes was monitored by dynein intermediate chain (DIC) and Cdk5Rap2 immunofluorescence. Cdk5Rap2 is a centrosomal protein (Fong *et al.*, 2008), and the Cdk5Rap2 antibody worked well to identify centrosomes in our staining conditions. The 74.1 DIC antibody works exceptionally well for immunofluorescence (IF) and immunoprecipitation (IP) of the entire dynein complex (Bingham *et al.*, 1998; Mesngon *et al.*, 2006), and is used throughout the study. In WT cells, exposure to insulin for 30 min or 1 h resulted in accumulation of dynein at centrosomes (as measured by a centrosome enrichment index [CEI]). The same accumulation was not observed in MIN cells. In fact, these cells had somewhat more dynein at centrosomes before addition of insulin but significantly reduced accumulation by 1 h of insulin exposure (Figure 1, E–G). That MIN cell CEI is reduced by insulin or by the GSK-3β inhibitor CT99021 is interesting and may be related to reports that GSK-3β can also inhibit kinesin (Morfini *et al.*, 2004; Weaver *et al.*, 2013; Dolma *et al.*, 2014). Kinesin stimulation would not be countered by dynein stimulation, resulting in a net decrease in CEI.

Because an overall lower number of dynein motors might contribute to the difference in response to insulin, we measured the level of dynein WT and MIN cell lysates (Supplemental Figure S1, A and B) In fact, the DIC bands in MIN cell extracts were somewhat more intense than in WT extracts. Moreover, we have observed that the dynein regulator, Ndel1, accumulates with dynein at centrosomes in response to insulin in WT but not MIN cells (Figure 1, H and I). Together these data indicate that the truncated MIN isoform of APC disrupts insulin's capacity to regulate dynein without interfering with its capacity to inhibit GSK-3β.

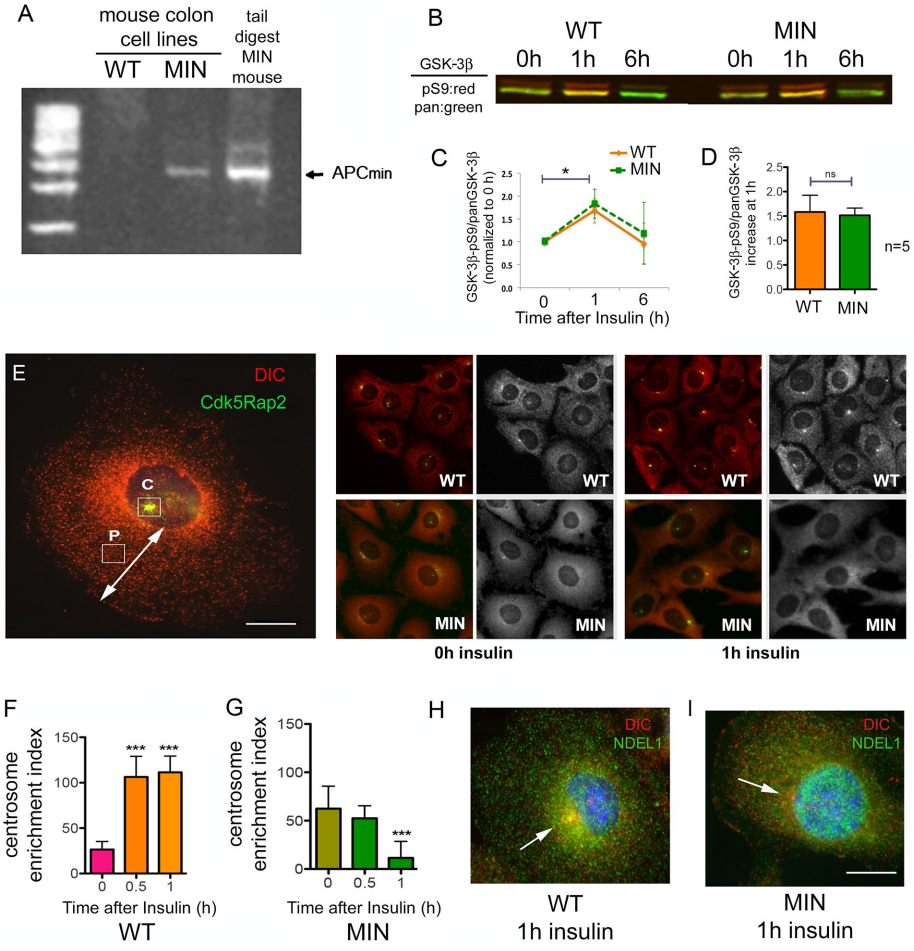


**FIGURE 1:** MIN cells respond differently to acute insulin exposure or GSK-3β inhibition after 12 h in starvation medium. (A) Primers for genotyping $APC^{+/MIN}$ mice were used to determine that the cell line derived from $APC^{+/min}$ mouse colon (MIN), but not the cell line derived from WT mice, expresses the truncated MIN isoform of APC. Sequencing indicated that the MIN cells retain one copy of the WT APC gene (unpublished data). (B) The ratio of inactivated GSK-3β (GSK-3β-pS9) to total GSK-3β (pan–GSK-3β) for WT and MIN cells exposed to 0, 1, or 6 h of insulin was determined by Western blot. Phospho-S9 antibody band, red; pan–GSK-3β band, green. (C) Li-Cor densitometry analysis of three Western blots shows mean ± 95% CI. $*p < 0.05$ by one-way ANOVA. (D) Average increase in S9/pan–GSK-3β after 1 h was determined from five Western blots. (E) Cdk5RAP2 IF (green) was used to label centrosomes in WT and MIN cells costained for DIC (red). Left, CEI calculated by subtracting the intensity of DIC fluorescence measured at a site halfway between the nucleus and the cell periphery (P) from the DIC intensity measured at the centrosome (C). Scale bar, 10 μm. Right, representative WT and MIN cells before and after insulin. The grayscale shows DIC only. (F, G) Acute insulin exposure to starved cells increased CEI in WT cells but not in MIN cells. Significance in C and D was determined with two-tailed paired Student's *t* test from three (C) or five (D) separate experiments. Significance in F and G was determined by ANOVA from four independent experiments, ~500 cells/condition. $***p < 0.001$. (H) A WT cell (left) exposed to insulin for 1 h shows accumulation of both DIC (red) and Ndel1 (green) at the centrosome. (I) This was not the case in MIN cells. Scale bar, 10 μm.

APC and GSK-3β both influence MT dynamics and stability (Zumbrunn *et al.*, 2001; Etienne-Manneville and Hall, 2003). Because changes in the MT cytoskeleton could lead to alterations in dynein distribution, we looked at the organization of MTs in starved WT and MIN cells with or without 1-h insulin treatment (Figure 2). Although there may be subtle differences, the four groups looked fairly similar at this level of analysis, supporting the idea that dynein activation, rather than a change in MT organization, was responsible for redistribution caused by acute insulin exposure to WT cells. We also examined the levels of three modified tubulin isoforms (tyrosinated, acetylated, and detyrosinated) in extracts from both cell lines. We observed no difference in overall levels of acetylated or tyrosinated tubulin by western blotting (Supplemental Figure S1, A and B). An antibody against detyrosinated tubulin (most frequently cited in recent reports) labeled a 50-kDa form less intensely in MIN cells than in WT cells. Recent reports indicate that dynein does not initiate transport as robustly on detyrosinated MTs, and vesicles bind less robustly to detyrosinated MTs (McKenney *et al.*, 2016; Nirschl *et al.*, 2016), so this is not likely to explain the *reduced* dynein stimulation in MIN cells.

Of interest, tyrosinated MTs in MIN cells tended to curve along the plasma membrane, whereas in WT cells, they tended to end more abruptly (Supplemental Figure S1, C–F). Acetylated MTs were only detected in a subset of cells (~12% of WT or MIN cells, with or without insulin). Unfortunately, the antibody raised against detyrosinated MTs detected multiple bands on a Western blot in addition a band of the appropriate size (unpublished data), and so any IF signal might be due to nonspecific interactions. However, MTs labeled with this antibody were often also positive for acetylated tubulin (Supplemental Figure S1, G–L). No obvious difference was observed between MIN and WT cells.

### GSK3 inhibition causes dynein release from the cell periphery in WT cells

CT99021 is a highly specific GSK-3β inhibitor (Eldar-Finkelman, 2002). CT99021 does not act through S9 phosphorylation but instead prevents an activating autophosphorylation of tyrosine 216, which was observed in our system by Western blotting with a phosphospecific antibody (Figure 3A). Direct pharmacological inhibition of GSK-3β with CT99021 for 1 h stimulated dynein centrosomal accumulation in WT cells but not in MIN cells (Figure 3B). Thus the presence of the MIN isoform also alters the dynein response to acute GSK-3β inhibition.

Reasoning that the source of newly activated, centrosomal-targeted dynein might be a pool that resides at MT plus ends or attached to the plasma membrane (Dujardin and Vallee, 2002; Markus *et al.*, 2009), we used IF in fixed WT cells to evaluate DIC and APC localization near the cell periphery. Commercial APC antibodies are not especially good for either IF or IP (Brocardo *et al.*, 2005); we used the APC-M2 antibody for all studies reported here (Wang *et al.*, 2009). Punctate APC and DIC staining was observed in the cytoplasm, and APC was also prominent in the nucleus (Figure 3C). Colocalization was visible throughout the cytoplasm, including at the cell periphery, where we focused our analyses (Figure 3D). The intensity of APC and dynein IF was measured along a line drawn at the edge of the cell in WT cells exposed to CT99021 for 1 h (Figure 3E). The dynein intensity but not the APC intensity was on average lower than in untreated cells,

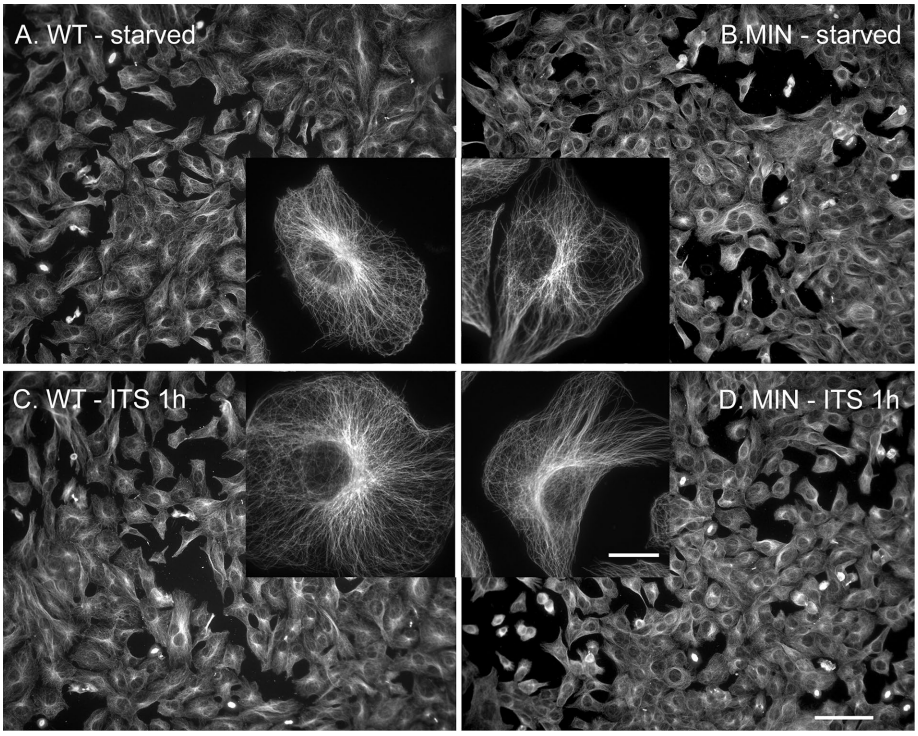


**FIGURE 2:** Microtubule organization is similar in WT and MIN cells with and without 1-h insulin exposure. Normal full culture medium was replaced with serum- and insulin-free medium for 12 h, and then insulin (ITS, 10 μM) was added for 1 h to one set of cultures. (A) WT cells and (B) MIN cells with no added insulin or (C) WT cells and (D) MIN cells that were exposed to insulin for 1 h were fixed and processed for α-tubulin IF. Insets, individual cells at higher magnification (63×). Scale bars, 50 μm (20× image), 10 μm (inset).

suggesting that dynein but not APC moved away from the cell membrane in response to the drug (Figure 3, F and G). We also examined dynein at the periphery in cells exposed to insulin. In this experiment, we measured the dynein intensity in the same way but compared WT and MIN cells exposed to insulin for 1 h. Substantial dynein immunoreactivity was observed in MIN cells but not in WT cells, indicating that although dynein can be present at the periphery, the insulin-dependent mechanism for release is not active in MIN cells (Figure 3H).

### Dynein and full-length APC can form a complex that is disrupted by the presence of the MIN isoform

The 2843–amino acid APC domain structure is shown in Figure 4A. The MIN mutation causes an early termination at amino acid 850 (Su *et al.*, 1992) but encompasses an oligomerization domain as well as Arm repeats that can associate with the APC membrane recruitment (AMER) family of membrane-associated proteins. AMER1 and 2 membrane-associated proteins can tether APC to the plasma membrane (Grohmann *et al.*, 2007; Tanneberger *et al.*, 2011). Missing in the MIN isoform are the 15–amino acid repeats, the SAMP and 20–amino acid repeats, the mutation cluster region (MCR), and binding sites for MTs, EB1, and PDZ domain–containing proteins.

Reports that APC and dynein function in some of the same cellular processes and are enriched at MT plus ends led to speculation of an interaction between these proteins (Mimori-Kiyosue and Tsukita, 2003). However, until now, this has not been observed or, to our knowledge, reported, possibly because of the paucity of useful APC antibodies. We reprobed a previously published dynein immunoprecipitate from WT mouse brain extracts (Gao *et al.*, 2015) using our APC-M2 antibody and found that full-length APC coprecipitated with dynein (Figure 4B). We also found that dynein coprecipitated with APC (Figure 4C). Of interest, GSK-3β was observed in both sets of IPs. In those experiments, beads only were used as a control, but a specific pull down of APC by dynein was also confirmed using mouse immunoglobulin G (IgG) as a nonspecific antibody (Figure 4D).

MIN mice express full-length APC protein from one allele and a truncated APC from the other. The amount of full-length APC in MIN brain extract is about half that in WT brain extract (Figure 4E). We repeated the dynein co-IP using brain extract derived from MIN mice and found that substantially less full-length APC coprecipitated with dynein than coimmunoprecipitated with dynein from WT brain (Figure 4F). Because the ratio of APC that coprecipitated with dynein in MIN versus WT brain extracts (Figure 4F) was less than the ratio of full-length APC protein in MIN versus WT brain extracts (Figure 4E), we hypothesize that the MIN isoform interferes with the interaction between dynein and full-length APC.

The MIN isoform of APC was not detected in MIN brain extracts (Figure 4E) because APC-M2 was raised against the more C-terminally located15–amino acid repeats, an epitope not present in this region (Wang *et al.*, 2009). We also tested two commercially available antibodies raised against the amino-terminal region of APC but were not able to reliably detect the MIN isoform. Both antibodies detected faint bands that were likely full-length APC in WT mouse brain and colon cell extracts but also labeled smaller polypeptides (unpublished data). In MIN cells, one of the antibodies detected a protein that was the appropriate size for the MIN isoform, but several smaller peptides were also observed, reducing confidence of specificity.

### A green fluorescent protein–tagged C-terminal APC fragment expressed in Cos-7 cells coimmunoprecipitates with endogenous dynein

The schematic in Figure 5A shows two APC fragments used in these experiments. The 746–amino acid N-terminal fragment of APC (nAPC) is similar to the MIN isoform, in that it contains the oligomerization domain and armadillo repeat region known to interact with AMER protein family members, but is missing the midregion and C-terminal domains. The 272–amino acid C-terminal fragment of APC (cAPC) covers the EB1 and PDZ-binding domains but does not contain the basic region that is most commonly shown to interact with MTs. However, one report demonstrated that a construct of a similar size to cAPC unexpectedly cosedimented with Taxol-stabilized MTs, pointing to the intriguing possibility of a second MT-binding site (Dikovskaya *et al.*, 2010). We used an enhanced green florescent protein (EGFP) vector to express EGFP-tagged full-length APC (FL-APC) as well as EGFP-tagged nAPC and cAPC. FL-APC was only observed in a very small percentage of cells, where it labeled MT-like structures in cellular protrusions (Figure 5B), as described by others (Mimori-Kiyosue *et al.*, 2000; Zumbrunn *et al.*, 2001). Some dynein immunoreactivity was observed at these protrusions (arrows, Figure 5B). nAPC was aggregated in cytoplasmic blebs, suggesting

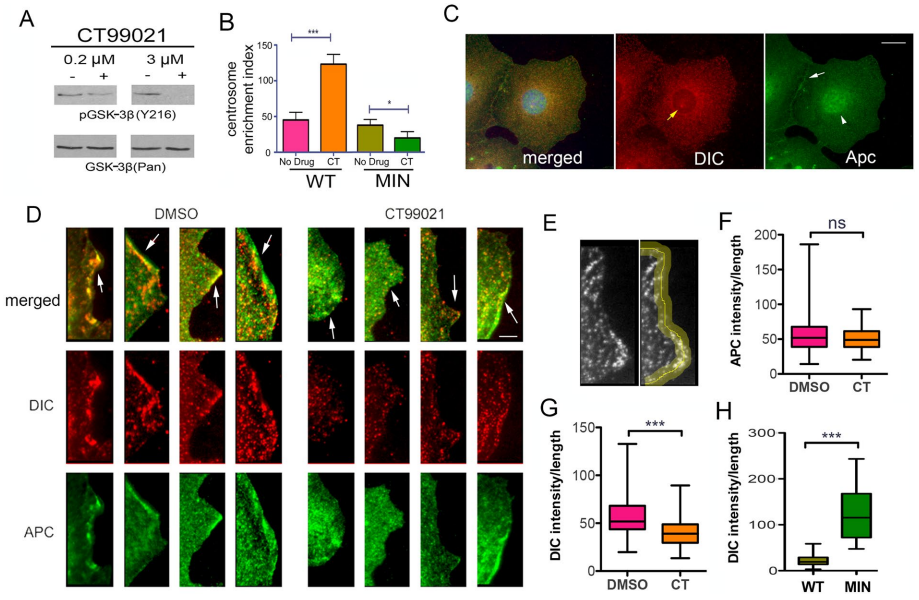


**FIGURE 3:** Dynein is reduced at the cell periphery in WT cells. (A) A GSK-3β inhibitor, CT99021 (CT), prevents an activating tyrosine (auto) phosphorylation (Y216). (B) Acute GSK-3β inhibition with CT also increased CEI in WT but not MIN cells. Significance determined by ANOVA from four independent experiments, ~500 cells/condition. *$p < 0.05$, ***$p < 0.001$ (C) Punctate APC (green) and DIC (red) IF occur throughout the cytoplasm in a WT cell. DIC can be seen at the centrosome (yellow arrow, middle). APC is more pronounced at cell junctions (white arrow, right) and in the nucleus (white arrowhead, right). Scale bar, 10 μm. (D) Digital enlargements of four WT cells treated with CT99021 for 1 h (right) and 4 untreated cells (left) reveal some overlap of DIC and APC at leading edges of the cell periphery (arrows). Scale bar, 5 μm. (E) Pixel intensities were measured along a 5-μm-wide line drawn at the cell peripheries of 74 interphase cells for each condition. (F, G) CT99021 reduced the average DIC pixel intensity but not the average APC intensity at the cell periphery. (H) Acute insulin exposure reduced the peripheral DIC intensity in WT but not MIN cells. Significance in F–H was determined using an unpaired two-tailed Student's *t* test from three independent experiments; 75 cells/condition. ***$p < 0.001$.

that it forms aggregates or other higher-order structures, as suggested by others (Schneikert *et al.*, 2011). A small amount of the tagged peptide, as well as a small amount of dynein, localized to cellular protrusions (arrow, Figure 5C) where they have the potential to interact with FL-APC. EGFP-cAPC was more diffusely distributed and may have subtly altered dynein distribution so that it too was more diffuse (Figure 5D). Both fragments appeared to reduce viability: fewer cells were present 24–48 h after transfection, and pyknotic nuclei were observed. Of interest, when both nAPC and cAPC were expressed at the same time, few if any EGFP aggregates were observed, suggesting that the C-terminal fragment affected the distribution or expression of the N-terminal fragment (unpublished data). Moreover, cell loss was exacerbated when the fragments were coexpressed (unpublished data), suggesting that aggregation of nAPC might be caused by the loss of the C-terminal domain and be somewhat protective.

We performed IP of endogenous dynein (Figure 5D). cAPC was specifically coprecipitated with dynein, but nAPC was also observed in the IgG control. Although there is a slightly stronger nAPC band in the dynein IP, we cannot conclude that this interaction is specific. We also performed anti-GFP co-IPs to examine proteins that may interact with nAPC and cAPC. Of interest, EGFP-cAPC, but not EGFP alone, reduced the amount of endogenous full-length APC that coprecipitated with dynein, suggesting that the fragment can compete with a binding site in the endogenous protein (Figure 5F). In another study, endogenous full-length APC coprecipitated with EGFP-nAPC but not EGFP-cAPC (Figure 5G). This supports the finding that the N-terminal domain is important for APC oligomerization (Nelson and Nathke, 2013) and suggests that the oligomerization domain is distinct from the dynein-binding domain.

### The interaction between APC and dynein is sensitive to GSK-3β activity

We showed previously that phosphorylation of dynein by GSK-3β reduced its binding to a regulatory protein, Ndel1 (Gao *et al.*, 2015). We therefore carried out a series of experiments to explore the role of GSK-3β in regulating the dynein–APC interaction. In contrast to Ndel1, treating WT or cAPC-expressing cells for 12 h with a GSK-3 inhibitor (CT99021) *reduced* the amount of endogenous full-length APC or EGFP-cAPC that coprecipitated with dynein (Figure 6, A and B). This was supported by experiments with a mutant EGFP-IC1B (M), engineered with S88A and T89E mutations in GSK-3β sites (Gao *et al.*, 2015), which substantially reduced the amount of endogenous APC compared with WT EGFP-IC1B (Figure 6C). That the cAPC interaction was sensitive to dynein phosphorylation by GSK-3β was also supported by experiments with purified proteins. A soluble histidine (His)-tagged C-terminal fragment of APC (his-cAPC) and purified bovine brain dynein were exposed to GSK-3β in an in vitro kinase assay. Several dynein subunits, but not cAPC, incorporated $\gamma$-$^{32}$P-ATP (Figure 6D). His-cAPC coprecipitated more robustly with phosphorylated bovine brain dynein (Figure 6, E and F). We cannot rule out that GSK-3β phosphorylation of other APC domains (Ferrarese *et al.*, 2007) are involved in regulating the dynein APC interaction. However, our data strongly suggest a significant contribution of dynein phosphorylation by the kinase.

### The MIN isoform alters the dynein response to the insulin sensitizer rosiglitazone in both cells and mouse colon

In our previous study, we demonstrated that exposing serum-starved WT mouse colon cells to rosiglitazone for 12 h produced the dynein-accumulation phenotype, and this was dependent on ongoing transcription (Gao *et al.*, 2015). Rosiglitazone is a PPARγ agonist, and its insulin-sensitizing properties are believed to be related to transcriptional changes caused by activation of this nuclear hormone receptor (Choi *et al.*, 2014). The dynein response to rosiglitazone did not occur in the absence of insulin and was mimicked by prolonged exposure to CT99021 (Gao *et al.*, 2015). Moreover, a constitutively active GSK-3β construct or pharmacological inhibition of AKT (a kinase that inhibits GSK-3β in the insulin pathway) blocked the response. This indicates that the dynein response was a consequence of increased insulin signaling.

Rosiglitazone has been considered as a candidate for chemotherapy and chemoprotection, but the results have been inconsistent, and there are side affects associated with the drug (Frohlich and Wahl, 2015). To determine whether the presence of cancer-causing mutations in APC can influence the dynein accumulation response to rosiglitazone, we tested the drug in MIN cells and

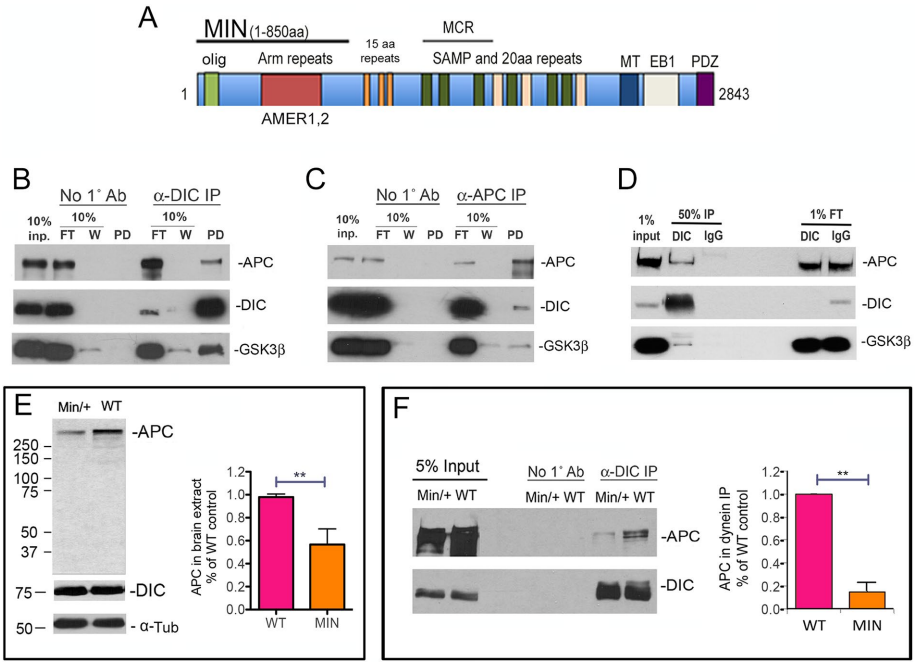


**FIGURE 4:** The MIN isoform interferes with an interaction between dynein and APC. (A) Domains in full-length APC and MIN APC. olig, oligomerization domain; Arm (armadillo) repeats interact with AMER membrane-associated proteins; 15–amino acid repeats are β-catenin–binding domains; MCR, mutation cluster region; SAMP and 20–amino acid repeats are important for Wnt signaling; MT, a basic region that confers microtubule binding; EB1, EB1-binding domain; PDZ, binding domain for PDZ-containing proteins. (B) Dynein was immunoprecipitated from WT mouse brain extract using the DIC 74.1 antibody. Both APC and GSK-3β were present in the immunoprecipitate but not in the no-antibody control (No 1° antibody). FT, flowthrough, that is, material that did not bind in the IP. W, material that was released from the IP in the first wash. (C) DIC and GSK-3β also coimmunoprecipitated specifically with APC pulled down by the APC-M2 antibody. (D) The dynein IP was repeated using mouse IgG as a nonspecific antibody control. Endogenous APC and GSK-3β coprecipitated specifically with the DIC immunoprecipitate but not the IgG immunoprecipitate. (E) By Western blotting, MIN brain extracts contain ~50% of the full-length APC in WT extracts, as quantified from four separate experiments. Significance was determined by paired two-tailed Student's *t* test, $^{**}p < 0.01$. The smaller MIN isoform is not detected with the APC-M2 antibody. DIC and α-tubulin (α-Tub) levels do not appear to be different. (F) Significantly less full-length APC coimmunoprecipitates with dynein from MIN brain extract. The amount of APC in DIC immunoprecipitates from WT and MIN brain extract was quantified from three separate experiments. Significance was determined by paired two-tailed Student's *t* test, $^{**}p < 0.01$.

found that they were unable to produce the dynein-accumulation phenotype (Figure 7, A and B), suggesting that insulin sensitization (or other rosiglitazone effects) cannot rescue the defect caused by the APC mutation. MIN and WT cells expressed equivalent levels of PPARγ, and receptor expression was not affected by the drug in either cell type, so the difference in dynein response is likely due to a defect in the insulin-sensitive dynein–APC interaction rather than a difference in the ability to respond to rosiglitazone (Figure 7B, inset). In our earlier study, we found that rosiglitazone also induced dynein accumulation in the HCT116 human cancer cell line (Gao *et al.*, 2015). This cell line has WT *APC* alleles, and carcinogenesis is believed to have arisen due to mutations in other genes (Dikovskaya *et al.*, 2007). Of interest, expression of EGFP-nAPC in these cells blocked the dynein response, providing support for the notion that the truncated APC isoform interferes with insulin-dependent dynein regulation (Figure 7C). There was no significant difference in the ratio of GSK-3β-pS9/total GSK-3β in response to rosiglitazone, indicating that signal transduction was functioning appropriately in these cells (Figure 7D).

We also visualized the distribution of phospho-AKT, which is the activated form of the protein. AKT is recruited to membranes early in the insulin-signaling pathway, where it becomes phosphorylated and activated to target its substrates, including GSK-3β. An increase in phospho-AKT at leading edges near the cell periphery was noted in both WT and MIN cells after rosiglitazone exposure (Figure 7E). This supports the conclusion that the insulin-signaling pathway is functional in the MIN cells but is unable to stimulate dynein movement.

Glitazones and other diabetes medications are being considered as potential chemotherapeutics (Chang *et al.*, 2012; Mendonca *et al.*, 2015; Ramjeesingh *et al.*, 2016). However, data from both human studies and experimental models can be confusing and sometimes contradictory. This may be related to unanticipated effects of the drugs. To determine whether acute administration of rosiglitazone could affect dynein distribution in intact colon cells, it was gavage fed to 8-wk-old WT mice and $APC^{+/min}$ littermates daily for 6 d. We examined crypts in young animals and in regions without adenomas, and so there is a strong likelihood that the cells have not lost heterozygosity for the MIN mutation. Animals were killed on day 6, and colonic crypts were examined for dynein distribution by immunofluorescence. Amazingly, dynein had accumulated at the apical surface in WT but not $APC^{+/min}$ crypts (Figure 7F). This is particularly exciting because MTs are oriented such that their minus ends are directed toward the apical surface. This indicates that, at least acutely, this class of drugs can affect cellular events that are controlled by dynein in vivo.

## DISCUSSION

Here we showed for the first time that APC and dynein can exist in a complex. We also provided evidence that tumorigenic mutations in APC interfere with this interaction. In addition to disrupting the APC–dynein interaction, mutant APC isoforms also disrupt an insulin-dependent change in dynein distribution.

We showed previously that dynein redistribution was linked to inhibition of GSK-3β activity and identified sites on dynein intermediate chains that are targeted by the kinase. We also showed that Ndel1, a dynein-binding protein that can increase dynein's force-generating capacity (McKenney *et al.*, 2010), interacts preferably with unphosphorylated dynein. CT99021 was able to stimulate dynein-dependent transport of acidic organelles. Here we provide evidence that unlike Ndel1, APC prefers to bind to phosphorylated dynein and propose a model in which a pool of phosphorylated dynein is retained at the plasma membrane by APC (Figure 8A). This scenario is plausible because APC can reportedly interact with membranes via association with AMER1/2 proteins (Grohmann *et al.*, 2007; Tanneberger *et al.*, 2011). Alternatively, dynein could be

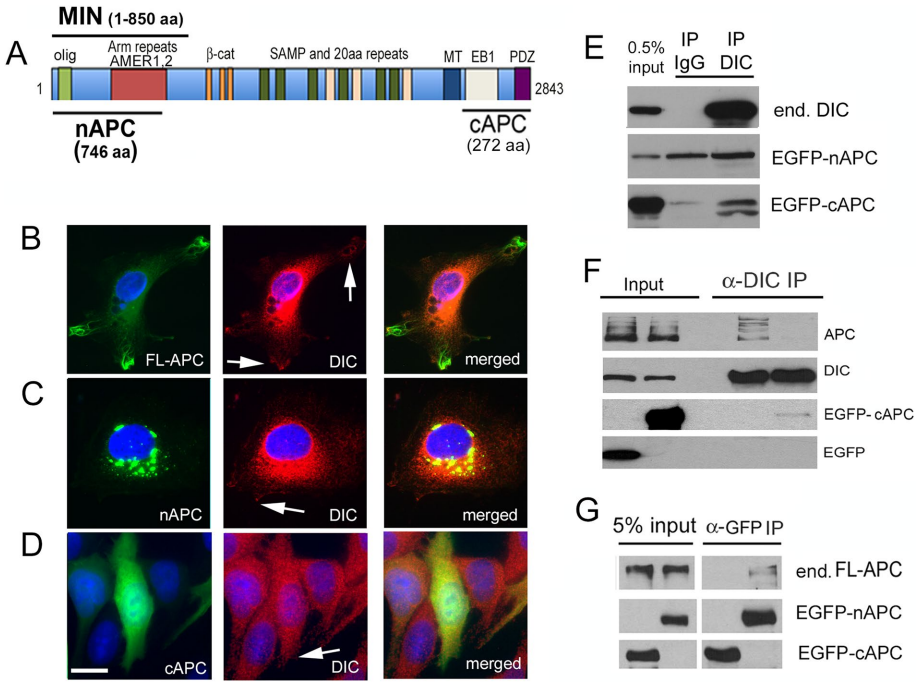


**FIGURE 5:** A C-terminal APC fragment expressed in Cos-7 cells coimmunoprecipitates with endogenous dynein. (A) Location of an N-terminal 746–amino acid APC fragment (nAPC) and a C-terminal 272–amino acid APC (cAPC) fragment used in several experiments. Also shown is the 850–amino acid MIN isoform. (B) Full-length APC fused to EGFP (green) transiently expressed in Cos-7 cells localizes along MTs in cellular protrusions. DIC (red) is concentrated in the cytoplasm but present near the peripheral regions of protrusions (arrows). (C) EGFP-nAPC (green) is enriched in large aggregates in the cytoplasm. Very small puncta of EGFP-nAPC associate with DIC (red) in cellular protrusions at the cell periphery (arrow). (D) EGFP-cAPC (green) is diffuse throughout the cytoplasm and is present in the nucleus. Scale bar, 10 μm. (E) Western blot of proteins in a dynein immunoprecipitate. Top, endogenous dynein (end. DIC) is precipitated by a dynein antibody but not by nonspecific mouse IgG. Middle, EGFP-nAPC is present in both the IgG and the DIC immunoprecipitate. Bottom, EGFP-cAPC coprecipitated specifically with dynein, not IgG. The lower anti-GFP–labeled band may be a proteolytic fragment or a modified peptide that is enriched in the DIC immunoprecipitate. (F) Transient expression of EGFP-cAPC, but not EGFP alone, reduced the amount of endogenous full-length APC (APC) that coprecipitated with dynein. (G) Endogenous APC (end. FL-APC) did not coprecipitate with EGFP-cAPC but did coprecipitate with EGFP-nAPC, which contains an oligomerization domain.

retained near the membrane by association of APC with a cadherin-linked pool of β-catenin (Sharma *et al.*, 2006). It is also possible that APC located at MT plus ends can "capture" dynein (Morrison, 2009). Indeed, all three could be true, given that APC, β-catenin, and dynein are likely to be important for MT capture near the cell cortex at leading edges of migrating cells and in mitotic spindle orientation (Dujardin and Vallee, 2002; Mimori-Kiyosue and Tsukita, 2003). How do APC and dynein get to the membrane or the plus ends? The C-terminal region of APC interacts with plus end–directed kinesin motors, which could drive the peripheral localization of APC in the cell (Jimbo *et al.*, 2002; Ruane *et al.*, 2016). Dynein is also ferried to plus-end locations by kinesin motors (Roberts *et al.*, 2014). Our dynein centrosome accumulation data suggest a model in which insulin signaling inactivates GSK-3β at or near the plasma membrane, creating an environment that favors dynein dephosphorylation. This environment would therefore favor Ndel1 binding over APC binding, effectively releasing some of the local pool of dynein to translocate along MTs toward minus ends (Figure 8B). APC is believed to form homodimers or oligomers, but it is not known whether this is required for dynein binding. In cells with cancer-causing APC truncations, the C-terminal domain is absent. We suspect that these APC isoforms form aggregates or other higher-order structures in the cytoplasm but that they also can interact with full-length APC and prevent dynein from binding, so the insulin-sensitive APC bound pool of dynein would not be available for activation. This would explain why no centrosome accumulation occurs in response to hormone binding to receptors. Substantial dynein immunoreactivity is present at the plasma membrane in MIN cells, so if our model is correct, there may be non–APC-dependent mechanisms underlying this distribution.

This model is likely too simplistic, given the complexities of intracellular signaling, especially those involving APC, insulin, and GSK-3β. Other events that could contribute to the altered dynein behavior, including direct effects of APC and GSK-3β on the MT cytoskeleton, are likely to affect insulin-dependent regulation of dynein (Zumbrunn *et al.*, 2001; Etienne-Manneville and Hall, 2003; Etienne-Manneville, 2010; Lui *et al.*, 2016a,b). The second MT-binding domain in the extreme C-terminal region of APC (Dikovskaya *et al.*, 2010; Gupta *et al.*, 2014) may play a role in controlling the APC–dynein interaction and the response to insulin signaling. We did not observe an obvious MT distribution pattern of cAPC-EGFP, and so this association might require some other regulatory factors in vivo. It will be interesting to determine whether GSK-3β alters the binding of cAPC fragments to MTs and affects MT capture at the cell cortex. The MIN mutation would not have this MT-binding capacity, which might affect the availability of MT tracks for dynein's insulin-dependent movement toward centrosomes. The overall organization of the MT array was similar in WT and MIN cells, but tyrosinated MTs seemed to end more abruptly at the cell cortex in WT cells, whereas they frequently curved along the periphery in MIN cells. Of interest, sliding of MTs along the cell cortex is attributed to dynein in *Saccharomyces cerevisiae* (Adames and Cooper, 2000). This underscores the importance of bringing the new idea of dynein regulation by insulin into our understanding of APC and GSK-3β biology, providing a hitherto-overlooked potential link to cancer. Although we have not queried this directly, altered dynein regulation might even contribute to some of the MT phenotypes linked to APC dysfunction.

Although diabetes is a risk factor for colorectal cancer (Guraya, 2015) and there is evidence that familial adenomatous polyposis increases the risk for diabetes (Nieuwenhuis *et al.*, 2012), our data with animal and cell models of course do not prove that dynein deregulation is responsible for these associations. However, the findings do raise interesting questions. For example, why would insulin signaling stimulate a minus end–directed motor in the intestine? Liver, fat, and nervous tissues are such important targets for insulin signaling that relatively little is known about insulin signaling in the gut. Unlike cultured MIN and WT colon cells, those residing in the gut epithelium

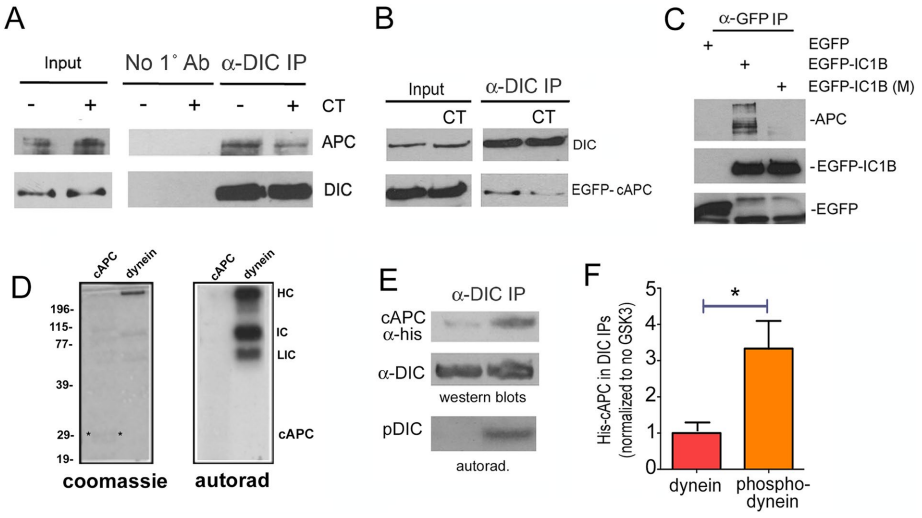


FIGURE 6: The interaction of dynein with the C-terminus of APC is modulated by GSK-3β activity and dynein phosphorylation. (A) A GSK-3β inhibitor CT99021 (CT) reduced the amount of endogenous APC that coprecipitated with endogenous dynein. (B) Similarly, less EGFP-cAPC coprecipitated with dynein from cells exposed to CT. (C) An EGFP antibody was used to pull down transiently expressed, EGFP-tagged dynein subunit IC1B. More endogenous APC coprecipitated with a WT construct than with an IC1B construct engineered with nonphosphorylatable S87A and T88V mutations in key GSK-3β sites, EGFP-IC1B (M). (D) Left, Coomassie-stained gel of histidine-tagged cAPC (cAPC) or purified bovine brain dynein (dynein). Both were exposed to purified GSK-3β in an in vitro kinase assay. Right, autoradiogram (autorad) shows γ-$^{32}$P-ATP incorporation in several dynein subunits but not in cAPC. HC, heavy chain; IC, intermediate chain; LIC, light intermediate chain. (E) His-tagged cAPC preferentially coprecipitated with dynein that had been previously phosphorylated by GSK-3β. (F) Quantitation of three separate IPs, average ± 95% CI. Significance was determined by paired two-tailed Student's *t* test, **p* < 0.05.

have a different MT arrangement, with minus ends located near the apical surface and plus ends enriched near basolateral membranes (Musch, 2004). This likely explains the accumulation of dynein at the apical surface when we treated mice with rosiglitazone. APC has been found at both apical and basolateral regions of human and mouse crypt cells, where it would be poised to tether dynein at plus ends (Miyashiro *et al.*, 1995; Senda *et al.*, 1996; Anderson *et al.*, 2002). Insulin receptors are also localized in the basolateral membrane (Ait-Omar *et al.*, 2011), and so dynein could theoretically control the internalization and trafficking of these receptors (or other proteins in this region) in response to high blood insulin levels. One study demonstrated that activation of insulin receptors located at the basolateral surface rapidly stimulated the MT-dependent translocation of an existing pool of PEPT1 transporters to the apical surface (Thamotharan *et al.*, 1999). Another study showed that deletion of intestinal epithelial insulin receptors attenuated a high-fat diet–induced elevation in cholesterol and increased mRNAs associated with stem cells, enteroendocrine cells, and Paneth cells (Andres *et al.*, 2015). Both could involve dynein-dependent trafficking.

From a cancer standpoint, it will be important to determine whether defects in dynein stimulation caused by APC mutations contribute to the development of intestinal cancers. This seems plausible, in that dynein function is vital not only for intracellular trafficking, but also for mitotic spindle dynamics, chromosome segregation, and cell migration (Steuer *et al.*, 1990; Dujardin and Vallee, 2002; Allan, 2011; Raaijmakers *et al.*, 2013). In the MIN mouse colon, mutant APC prevented dynein redistribution caused by rosiglitazone. Even if we consider only this defect in trafficking, loss of normal dynein control mechanisms could alter the uptake of nutrients from the luminal surface or impair the secretion of mucus from goblet cells and antimicrobial granules from Paneth cells. These latter events could alter the gut microbiome, which could affect carcinogenesis (Pfalzer *et al.*, 2016; Vogtmann *et al.*, 2016).

Many extracellular signals lead to GSK-3β inhibition, and there are multiple complex feedback loops that control kinase activity (Beurel *et al.*, 2015). It is interesting to speculate that the GSK-3β switch could be a universal scheme adopted by cells to drive minus-end trafficking in response to extracellular signals. If so, how is specificity achieved for specific trafficking events, and how is the duration of the dynein stimulation regulated? Could there be feedback loops that shut down the signal, and could these be specific for different extracellular ligands? Most studies indicate that the mechanisms promoting Wnt- versus insulin-induced GSK-3β inhibition are distinct, and this may be one way that cells avoid a potentially harmful activation of Wnt signaling by insulin and vice versa (Mendonca *et al.*, 2015; Zhou *et al.*, 2015). Future studies will aim at determining whether acute Wnt signaling affects dynein in the same manner as insulin. Finally, we need to consider all other known targets of GSK-3β that might be simultaneously affected when the kinase is inhibited, including APC itself and, of importance, the plus end–directed motor, kinesin (Pigino *et al.*, 2003; Morfini *et al.*, 2004; Weaver *et al.*, 2013; Dolma *et al.*, 2014). Clearly, there will be many twists and turns in the road before a complete understanding of GSK-3β regulated trafficking is attained.

## MATERIALS AND METHODS

### Cell lines

The murine young adult mouse colon (YAMC) epithelial cell line was derived from the colonic mucosa of a transgenic mouse generated by the introduction of a temperature-sensitive, interferon-inducible, SV40 T Ag, tsA58 (Immortomouse; Whitehead *et al.*, 1993). We refer to this line as WT in this article. The Immortomouse colon epithelial cell line (IMCE) was derived from the progeny of a cross between the Immortomouse strain and the Apc (min/+) mouse strain (Whitehead and Joseph, 1994). We refer to these as MIN cells. Both cell lines were first obtained from the Center for Colon Cancer Research at the University of South Carolina and later from a new batch from R. H. Whitehead (Vanderbilt University Medical Center). Cell lines were validated by genotyping and PCR. Cells were maintained at the permissive temperature (33°C) in full RPMI 1640 medium (2 mM glutamine, 10% fetal bovine serum [FBS], 0.5 U/ml penicillin, 100 μg/ml streptomycin, 5 U/ml murine γ-interferon, and 1% ITS [insulin, transferrin, and selenium; Cellgro]). Cos-7 cells and SW480 cells were maintained in full DMEM medium (2 mM glutamine, 10% FBS, 0.5 U/ml penicillin, and 100 μg/ml streptomycin). Cell lines were tested frequently for mycoplasma contamination using a mycoplasma detection kit from Thermo Fisher Scientific.

### Expression constructs and transfection

EGFP-nAPC was generated by cloning a *Bsp*EI and *Hin*dIII fragment of full-length human APC into a pEGFP C1 vector. cAPC was

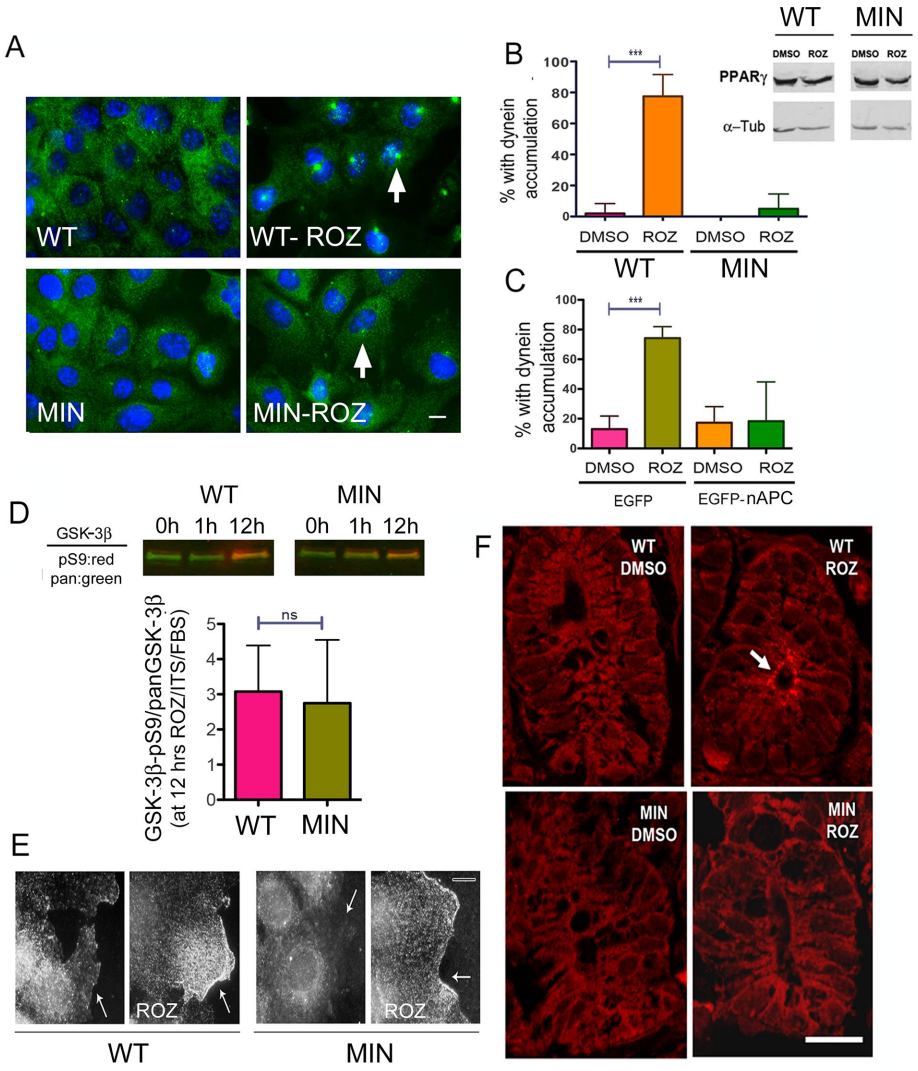


**FIGURE 7:** The MIN mutation alters the dynein distribution response to rosiglitazone (ROZ) in vivo. (A, B) A 12-h exposure of starved cells to serum plus ITS and ROZ causes DIC (green) to accumulate at centrosomes in WT but not MIN cells. Treatment of WT or MIN cells with ROZ does not lead to an increase in PPARγ expression (top, Western blots). (C) ROZ-induced dynein accumulation is also defective if EGFP-nAPC isoform is transiently expressed in HCT116 cells. (D) Inhibition of GSK-3β is detected after 12 h of ROZ treatment in both WT and MIN cells. (E) Phospho-AKT immunoreactivity is observed at the cell periphery (arrows) in both cell types after ROZ treatment. (F) Colonic crypts from WT but not MIN mice showed an alteration in DIC distribution (red) after 6 d of gavage-administered rosiglitazone. Significant differences in B and C were determined by ANOVA from three separate experiments, 75 cells/treatment; ***$p < 0.001$. Lack of a significant difference in D was determined by the paired two-tailed Student's *t* test from five experiments. ns, not significantly different.

generated by PCR amplification of a 747–base pair fragment of the 3′ end of full-length human APC. An *Eco*R1 and *Bam*H1 fragment was subcloned into a pET 30 EK/LIC vector (Novagen) for expression in *Escherichia coli* or the pEGFP-C1 vector for mammalian expression. The rat EGFP-IC1B construct was kindly provided by Kevin Pfister (University of Virginia, Charlottesville, VA). The IC1B mutant was described in Gao *et al.* (2015). All constructs were verified by sequencing. Cells were transfected using Lipofectamine 2000 or 3000 (Invitrogen) according to the manufacturer's directions.

### Antibodies

We used the following antibodies: CDK5RAP2 rabbit polyclonal antibody (pAb; Millipore), DIC mouse monoclonal antibody (mAb; 74.1; Santa Cruz Biotechnology), APC-M2 rabbit pAb (raised against the 15–amino acid repeat region; described in Wang *et al.*, 2009), DIC mouse mAb (74.1; Santa Cruz Biotechnology), GSK-3β mouse mAb (3D10; Cell Signaling Technology), phospho–GSK-3β (Ser-9) rabbit pAb (5B3; Cell Signaling Technology), GFP rabbit pAb (Ab290; Abcam), His-probe rabbit pAb (H-3; Santa Cruz Biotechnology), PPARγ1 rabbit pAb (H100; Santa Cruz Biotechnology), detyrosinated α-tubulin rabbit pAb (ab48389; Abcam), tyrosinated tubulin mouse mAb (TUB1A2; Sigma-Aldrich); acetylated tubulin mouse mAb (Clone 6-11-B1; Sigma-Aldrich); and α-tubulin mAb (T5168; Sigma-Aldrich).

### Measuring GSK-3β inhibition

PAGE was performed on WT and MIN cell extracts. Proteins were then transferred to nitrocellulose membrane. Membranes were blocked using Li-Cor Odyssey TBS Blocking Buffer and then probed with a mouse mAb to pan-GSK-3β and rabbit mAb to phospho–GSK-3β (serine 9), both at 1:1000. Li-Cor IRDye 680LT donkey anti-rabbit and 800CW donkey anti-mouse secondary antibodies were diluted in the Odyssey blocking buffer at 1:10,000. The membrane was then imaged using the Li-Cor Odyssey Sa system, and band intensities were measured using ImageStudio software.

### Effect of drugs on protein distribution and MT organization in cell lines

Cells were plated onto 12-mm glass coverslips in 24-well plates before drug treatment or transfection. For Figures 1, 2, and 3, D and E, and Supplemental Figures S1 and S2, cells were cultured for 12 h in medium without FBS or ITS in order to obtain maximum sensitivity to insulin (starved). Then, 1% ITS (Cellgro) or 3 μM CT99021 (Cayman Chemicals) was added for the indicated times. For Figures 3, A–C, and 7, A–C, after starvation, cells were exposed to 3 μm CT or 10 μM rosiglitazone (Biomol) for 12 h in full medium (containing both ITS and FBS). Cells were fixed and then processed for IF. For DIC, APC, or Ndel1 antibodies, cells were fixed in100% ice-cold methanol for 2 min; for tubulin and AKT antibodies cells, were fixed in warm 4% paraformaldehyde for 20 min followed by permeabilization with 0.2% Triton X-100 for 10 min. Nuclei were visualized using Hoechst dye (33258; Sigma-Aldrich). Coverslips were mounted onto glass slides using ProLong Gold Antifade (Invitrogen). Cells were visualized with an Axiovert 200 inverted microscope (Carl Zeiss) using Plan-Neo 100×/1.30 or Plan-Apo 63×/1.40 oil-immersion objectives (Immersol 518F; Carl Zeiss) or a Plan-Neofluor 20× dry objective.

### Protein interaction studies in mouse tissues

For Figure 4, B and F, Adult mouse brains were Dounce-homogenized in 50 mM Tris, pH 7.5, 0.1% NP-40, 100 mM NaCl, 1 mM

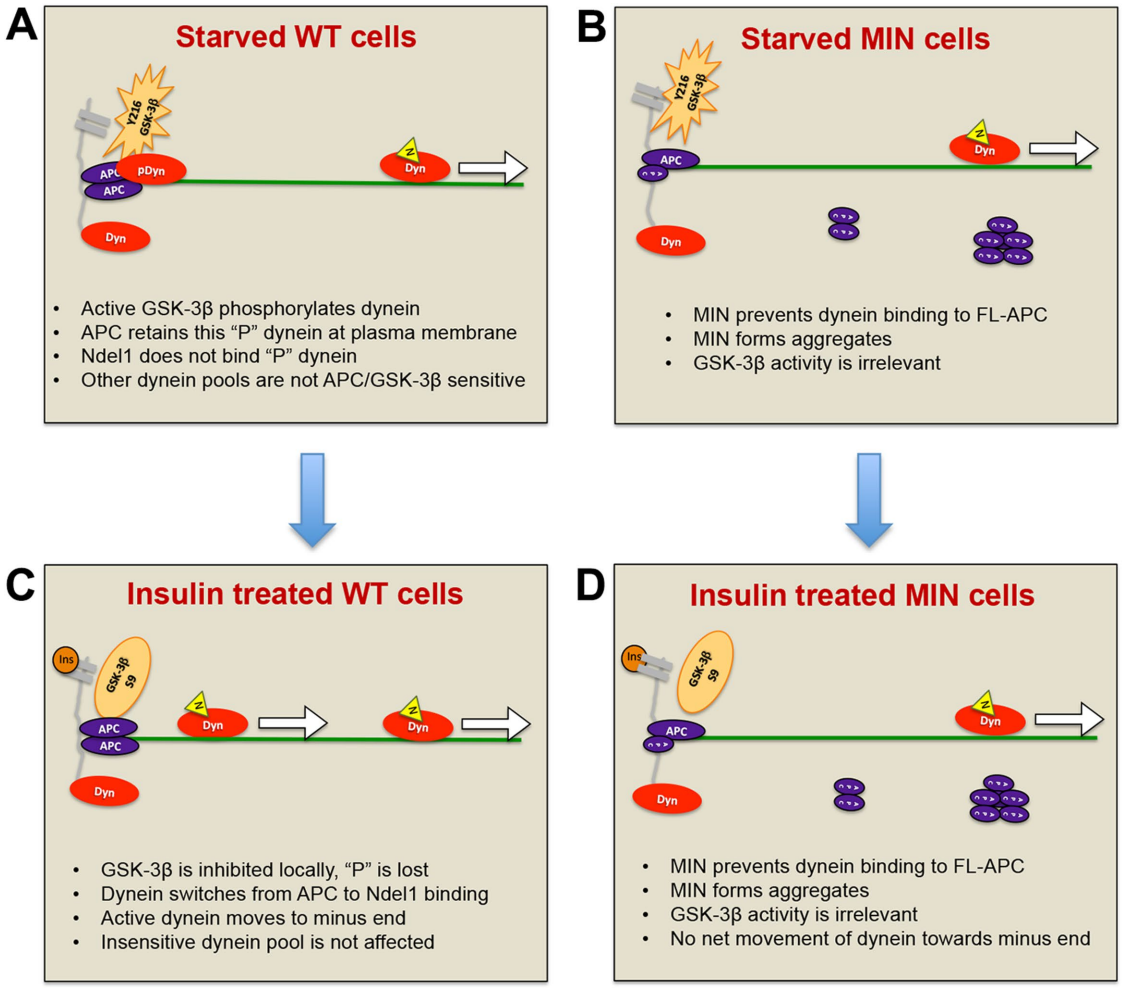


FIGURE 8: Model for how APC mutations affect insulin-induced dynein movement toward MT minus ends. (A) WT cells in the absence of insulin or serum factors: GSK-3β (orange star) near the membrane (gray) is phosphorylated on Y216 and active. Nearby dynein motors are phosphorylated, rendering them more likely to bind to APC than to Ndel1. Here phosphorylated dynein (pDyn, red oval) is shown bound to an APC homodimer (purple ovals) at sites of MT (green line) capture at the plasma membrane. Unphosphorylated dynein (Dyn) may be bound to Ndel1 (yellow triangle) and actively translocating (arrow). (B) Insulin (dark orange circle) binds to receptors, activating a signaling pathway that locally and transiently inactivates GSK-3β by S9 phosphorylation. Dynein becomes locally and transiently dephosphorylated, is released from APC, binds to Ndel1, and then moves toward MT minus ends. The increase in number of processive dyneins results in minus-end accumulation at centrosomes (not shown). (C) MIN cells in the absence of insulin or serum factors: GSK-3β is active, but there is a reduced pool of dynein associated with FL-APC because MIN APC blocks the interaction. MIN APC also forms aggregates in the cytoplasm. (D) Normal inhibition of GSK3β occurs in response to insulin signaling but as the APC-bound, insulin-sensitive pool of dynein is reduced, the net effect of insulin on motor distribution is minimal.

$MgCl_2$, 5 mM EDTA, protease inhibitor cocktail (Fisher), and Halt phosphatase inhibitor cocktail (Fisher). The lysates were incubated on ice for 30 min and then centrifuged at 17,000 × *g* for 30 min at 4°C. DIC or APC-M2 antibodies were incubated with Protein-A Dynabeads (Invitrogen) for 2 h at room temperature. Beads were washed twice with lysis buffer and then incubated overnight at 4°C with cell or tissue extract. Beads were then washed twice with lysis buffer and twice with PBS-T (phosphate-buffered saline with 0.1% Tween-20) at 4°C. Samples were eluted in 60 µl of PBS plus 20 µl of 6× sample buffer, boiled briefly, and then separated by SDS–PAGE and analyzed by Western blotting. For the DIC IP with IgG as a control (Figure 4D), lysis buffer also contained 10% glycerol, and extracts were centrifuged at 50,000 × *g* for 30 min. Lysates were incubated overnight with agarose beads conjugated to DIC antibody or normal mouse IgG (Santa Cruz Biotechnology). Beads were washed extensively in lysis buffer and PBST and then processed for SDS–PAGE. For all IPs involving endogenous APC, half of the sample was transferred to nitrocellulose for APC probing and the other half to polyvinylidene fluoride (PVDF) for DIC probing. Blots were incubated with primary antibodies overnight at 4°C and then exposed to the appropriate horseradish peroxidase–conjugated secondary antibodies. Labeled proteins were detected using chemiluminescence. Band intensities were determined using ImageJ Fiji image analysis software.

### Protein interaction studies in cells

Cos-7 cells were used because of the difficulty in transfecting the WT and MIN colon cell lines. Cells were transfected with EGFP,

EGFP-nAPC, EGFP-cAPC, or EGFP-IC1B constructs. For Figure 5E, after 16 h, cells were starved for 4 h, lysed in the lysis buffer on ice for 30 min, and then centrifuged at 50,000 × *g* for 30 min. Cell lysates were incubated overnight with agarose beads conjugated to DIC antibody or normal mouse IgG (Santa Cruz Biotechnology). Beads were washed extensively in 50 mM Tris, pH 7.5, 0.5% NP-40, 0.1% Triton X-100, 125 mM NaCl, 1 mM $MgCl_2$, and 5 mM EDTA and then in PBST, and then processed for SDS–PAGE and Western blotting. For Figures 5, F and G, and 6C, lysates were prepared 24–36 h after transfection and no starvation step was included. Lysates were sonicated for 10 pulses at level 1 with 10% output three times, incubated on ice for 10 min, and then centrifuged at 17,000 × *g* for 20 min at 4°C. Cell lysates were incubated overnight with agarose beads conjugated to DIC antibody or protein A beads alone. For Figure 6B, after transfection, cells were starved for 12 h and then exposed to 3 µM CT99021 for 12 h in full medium (containing both ITS and FBS).

### Protein interaction studies with purified proteins

Bacterial extract containing His-tagged c-APC was used in dynein co-IPs. Cytoplasmic dynein was purified from bovine brain as described previously (Bingham *et al.*, 1998). The dynein contains all subunits in the motor holoenzyme, and the prep contains no detectable Lis1, p150 glued, Ndel1, EB1, or tubulin (Mesngon *et al.*, 2006). The purified brain dynein was first incubated overnight with 74.1 mouse monoclonal IC antibody-conjugated agarose beads (IC-Beads; Santa Cruz Biotechnology) in PBS-T with protease and phosphatase inhibitors. Beads were washed twice with PBS-T and once with 1× kinase buffer. Beads were incubated in $^{32}$P-γATP with or without GSK-3β at 37°C for 1 h. Beads were spun down and washed with PBS-T twice and then with PHM-T buffer (60 mM 1,4-piperazinediethanesulfonic acid, 25 mM 4-(2-hydroxyethyl)-1-piperazineethanesulfonic acid, 4 mM $MgSO_4$, 0.1% Tween 20, pH 6.9) and then were incubated with 500 µl of the cAPC-containing bacterial lysate. Beads were washed three times with PHM-T buffer and eluted in 60 µl of PBS plus 20 µl of 6× sample buffer. Proteins were separating by SDS–PAGE and transferred to PVDF membrane. Blots were exposed to autoradiography film (Denville) overnight at –80°C before probing for DIC and His tag.

### Rosiglitazone treatment of mice

C57BL6/J Apc (min/+) mice, originally obtained from Jackson Labs, were maintained in the Mouse Core Facility of the Center for Colon Cancer Research at the University of South Carolina. Apc (min/+) males were bred with C57BL6/J WT females, and heterozygous progeny were genotyped by PCR analysis of tail genomic DNA using allele-specific primers (Murphy *et al.*, 2004). Three WT and three Apc (min/+) adult male mice (4 wk) were gavage-fed rosiglitazone (Biomol) at a dose of 10 mg/kg body weight daily for 6 d. Three mice received a similar regimen of vehicle only (dimethyl sulfoxide). Jejunal segments were fixed in 3% paraformaldehyde and embedded in paraffin, sectioned, and placed on glass slides. Slides were heated in 10 mM citrate buffer, pH 6.0, for 10 min for antigen retrieval. Sections were incubated with the 74.1 DIC antibody for 2 h at room temperature and then washed and incubated with Alexa Fluor 568–conjugated goat anti-mouse secondary antibody (Molecular Probes) for 1 h. Sections were coverslipped using ProLong Gold Anti-Fade and then visualized with a Zeiss AxioImager M2 using an EC Plan-Neofluar 40×/1.30 oil-immersion objective. Digital images were acquired with a charge-coupled device camera linked to AxioVision software (Carl Zeiss).

### Statistics

All analyses were carried out using GraphPad Prism, version 5.00 for Mac OSX. In most of the figures, error bars represent ±95% confidence interval (CI). One-way analysis of variance (ANOVA) with Tukey's multiple comparison tests or paired or unpaired, two-tailed Student's *t* test were used as indicated in the figure legends. Immunofluorescence measurements were made using ImageJ Fiji software. For dynein accumulation experiments, 50 interphase cells were analyzed for each condition, and the percentages from three experiments ($N = 3$) were used to determine the mean (±95% CI) and the significance of the observed differences. Thus, for most bar graphs, the data were derived from 150 cells/condition. In other experiments, mean pixel intensities of DIC staining at centrosomes minus pixel intensities of DIC at a more peripheral site were compared for the whole population (150 cells) using $N = 150$. For graphs from Western blots, at least three repeats of the experiments were performed.

## ACKNOWLEDGMENTS

We are grateful to Stephen J. King for supplying purified bovine brain dynein and Kevin K. Pfister for providing the EGFP-IC1B construct. Cancer cell lines were provided by the University of South Carolina Center for Colon Cancer Research. We thank Steven P. Gross for critical review of the manuscript. This work was supported by National Institutes of Health Grants 5P20 RR017698 and R01 NS056314 and a grant from the Cancer Research and Prevention Foundation.

## REFERENCES

Adames NR, Cooper JA (2000). Microtubule interactions with the cell cortex causing nuclear movements in Saccharomyces cerevisiae. J Cell Biol 149, 863–874.

Ait-Omar A, Monteiro-Sepulveda M, Poitou C, Le Gall M, Cotillard A, Gilet J, Garbin K, Houllier A, Chateau D, Lacombe A, *et al.* (2011). GLUT2 accumulation in enterocyte apical and intracellular membranes: a study in morbidly obese human subjects and ob/ob and high fat-fed mice. Diabetes 60, 2598–2607.

Allan VJ (2011). Cytoplasmic dynein. Biochem Soc Trans 39, 1169–1178.

Anderson CB, Neufeld KL, White RL (2002). Subcellular distribution of Wnt pathway proteins in normal and neoplastic colon. Proc Natl Acad Sci USA 99, 8683–8688.

Andres SF, Santoro MA, Mah AT, Keku JA, Bortvedt AE, Blue RE, Lund PK (2015). Deletion of intestinal epithelial insulin receptor attenuates high-fat diet-induced elevations in cholesterol and stem, enteroendocrine, and Paneth cell mRNAs. Am J Physiol Gastrointest Liver Physiol 308, G100–G111.

Bahmanyar S, Nelson WJ, Barth AI (2009). Role of APC and its binding partners in regulating microtubules in mitosis. Adv Exp Med Biol 656, 65–74.

Barth AI, Caro-Gonzalez HY, Nelson WJ (2008). Role of adenomatous polyposis coli (APC) and microtubules in directional cell migration and neuronal polarization. Semin Cell Dev Biol 19, 245–251.

Barth AI, Siemers KA, Nelson WJ (2002). Dissecting interactions between EB1, microtubules and APC in cortical clusters at the plasma membrane. J Cell Sci 115, 1583–1590.

Berrueta L, Tirnauer JS, Schuyler SC, Pellman D, Bierer BE (1999). The APC-associated protein EB1 associates with components of the dynactin complex and cytoplasmic dynein intermediate chain. Curr Biol 9, 425–428.

Beurel E, Grieco SF, Jope RS (2015). Glycogen synthase kinase-3 (GSK3): regulation, actions, and diseases. Pharmacol Ther 148, 114–131.

Bingham JB, King SJ, Schroer TA (1998). Purification of dynactin and dynein from brain tissue. Methods Enzymol 298, 171–184.

Brocardo M, Nathke IS, Henderson BR (2005). Redefining the subcellular location and transport of APC: new insights using a panel of antibodies. EMBO Rep 6, 184–190.

Chang CH, Lin JW, Wu LC, Lai MS, Chuang LM, Chan KA (2012). Association of thiazolidinediones with liver cancer and colorectal cancer in type 2 diabetes mellitus. Hepatology 55, 1462–1472.
Choi SS, Park J, Choi JH (2014). Revisiting PPARgamma as a target for the treatment of metabolic disorders. EMBO Rep 47, 599–608.
Dikovskaya D, Li Z, Newton IP, Davidson I, Hutchins JR, Kalab P, Clarke PR, Nathke IS (2010). Microtubule assembly by the Apc protein is regulated by importin-beta–RanGTP. J Cell Sci 123, 736–746.
Dikovskaya D, Schiffmann D, Newton IP, Oakley A, Kroboth K, Sansom O, Jamieson TJ, Meniel V, Clarke A, Nathke IS (2007). Loss of APC induces polyploidy as a result of a combination of defects in mitosis and apoptosis. J Cell Biol 176, 183–195.
Dolma K, Iacobucci GJ, Hong Zheng K, Shandilya J, Toska E 2nd, White JA, Spina E, Gunawardena S (2014). Presenilin influences glycogen synthase kinase-3 beta (GSK-3beta) for kinesin-1 and dynein function during axonal transport. Hum Mol Genet 23, 1121–1133.
Dujardin DL, Vallee RB (2002). Dynein at the cortex. Curr Opin Cell Biol 14, 44–49.
Eldar-Finkelman H (2002). Glycogen synthase kinase 3: an emerging therapeutic target. Trends Mol Med 8, 126–132.
Etienne-Manneville S (2009). APC in cell migration. Adv Exp Med Biol 656, 30–40.
Etienne-Manneville S (2010). From signaling pathways to microtubule dynamics: the key players. Curr Opin Cell Biol 22, 104–111.
Etienne-Manneville S, Hall A (2003). Cdc42 regulates GSK-3beta and adenomatous polyposis coli to control cell polarity. Nature 421, 753–756.
Ferrarese A, Marin O, Bustos VH, Venerando A, Antonelli M, Allende JE, Pinna LA (2007). Chemical dissection of the APC Repeat 3 multistep phosphorylation by the concerted action of protein kinases CK1 and GSK3. Biochemistry 46, 11902–11910.
Fleming ES, Temchin M, Wu Q, Maggio-Price L, Tirnauer JS (2009). Spindle misorientation in tumors from APC(min/+) mice. Mol Carcinog 48, 592–598.
Fong KW, Choi YK, Rattner JB, Qi RZ (2008). CDK5RAP2 is a pericentriolar protein that functions in centrosomal attachment of the gamma-tubulin ring complex. Mol Biol Cell 19, 115–125.
Friedrich T, Richter B, Gaiser T, Weiss C, Janssen KP, Einwachter H, Schmid RM, Ebert MP, Burgermeister E (2013). Deficiency of caveolin-1 in Apc(min/+) mice promotes colorectal tumorigenesis. Carcinogenesis 34, 2109–2118.
Frohlich E, Wahl R (2015). Chemotherapy and chemoprevention by thiazolidinediones. Biomed Res Int 2015, 845340.
Gao FJ, Hebbar S, Gao XA, Alexander M, Pandey JP, Walla MD, Cotham WE, King SJ, Smith DS (2015). GSK-3beta phosphorylation of cytoplasmic dynein reduces Ndel1 binding to intermediate chains and alters dynein motility. Traffic 16, 941–961.
Grohmann A, Tanneberger K, Alzner A, Schneikert J, Behrens J (2007). AMER1 regulates the distribution of the tumor suppressor APC between microtubules and the plasma membrane. J Cell Sci 120, 3738–3747.
Gupta KK, Alberico EO, Nathke IS, Goodson HV (2014). Promoting microtubule assembly: a hypothesis for the functional significance of the +TIP network. Bioessays 36, 818–826.
Gupta RA, Dubois RN (2002). Controversy: PPARgamma as a target for treatment of colorectal cancer. Am J Physiol Gastrointest Liver Physiol 283, G266–G269.
Guraya SY (2015). Association of type 2 diabetes mellitus and the risk of colorectal cancer: a meta-analysis and systematic review. World J Gastroenterol 21, 6026–6031.
Hancock WO (2014). Bidirectional cargo transport: moving beyond tug of war. Nat Rev Mol Cell Biol 15, 615–628.
Hanson CA, Miller JR (2005). Non-traditional roles for the adenomatous polyposis coli (APC) tumor suppressor protein. Gene 361, 1–12.
He XK, Su TT, Si JM, Sun LM (2016). Metformin is associated with slightly reduced risk of colorectal cancer and moderate survival benefits in diabetes mellitus: a meta-analysis. Medicine 95, e2749.
Hendricks AG, Lazarus JE, Perlson E, Gardner MK, Odde DJ, Goldman YE, Holzbaur EL (2012). Dynein tethers and stabilizes dynamic microtubule plus ends. Curr Biol 22, 632–637.
Hunt SD, Stephens DJ (2011). The role of motor proteins in endosomal sorting. Biochem Soc Trans 39, 1179–1184.
Jimbo T, Kawasaki Y, Koyama R, Sato R, Takada S, Haraguchi K, Akiyama T (2002). Identification of a link between the tumour suppressor APC and the kinesin superfamily. Nat Cell Biol 4, 323–327.
Larsson SC, Orsini N, Wolk A (2005). Diabetes mellitus and risk of colorectal cancer: a meta-analysis. J Natl Cancer Inst Monogr 97, 1679–1687.
Lefebvre AM, Chen I, Desreumaux P, Najib J, Fruchart JC, Geboes K, Briggs M, Heyman R, Auwerx J (1998). Activation of the peroxisome proliferator-activated receptor gamma promotes the development of colon tumors in C57BL/6J-APCMin/+ mice. Nat Med 4, 1053–1057.
Ligon LA, Shelly SS, Tokito MK, Holzbaur EL (2006). Microtubule binding proteins CLIP-170, EB1, and p150Glued form distinct plus-end complexes. FEBS Lett 580, 1327–1332.
Lui C, Ashton C, Sharma M, Brocardo MG, Henderson BR (2016a). APC functions at the centrosome to stimulate microtubule growth. Int J Biochem Cell Biol 70, 39–47.
Lui C, Mok MT, Henderson BR (2016b). Characterization of adenomatous polyposis coli protein dynamics and localization at the centrosome. Cancers 8, E47.
Malek M, Aghili R, Emami Z, Khamseh ME (2013). Risk of cancer in diabetes: the effect of metformin. ISRN Endocrinol 2013, 636927.
Marin HE, Peraza MA, Billin AN, Willson TM, Ward JM, Kennett MJ, Gonzalez FJ, Peters JM (2006). Ligand activation of peroxisome proliferator-activated receptor beta inhibits colon carcinogenesis. Cancer Res 66, 4394–4401.
Markus SM, Punch JJ, Lee WL (2009). Motor- and tail-dependent targeting of dynein to microtubule plus ends and the cell cortex. Curr Biol 19, 196–205.
McKenney RJ, Huynh W, Vale RD, Sirajuddin M (2016). Tyrosination of alpha-tubulin controls the initiation of processive dynein-dynactin motility. EMBO J 35, 1175–1185.
McKenney RJ, Vershinin M, Kunwar A, Vallee RB, Gross SP (2010). LIS1 and NudE induce a persistent dynein force-producing state. Cell 141, 304–314.
Mendonca FM, de Sousa FR, Barbosa AL, Martins SC, Araujo RL, Soares R, Abreu C (2015). Metabolic syndrome and risk of cancer: which link? Metabolism 64, 182–189.
Mesngon MT, Tarricone C, Hebbar S, Guillotte AM, Schmitt EW, Lanier L, Musacchio A, King SJ, Smith DS (2006). Regulation of cytoplasmic dynein ATPase by Lis1. J Neurosci 26, 2132–2139.
Mimori-Kiyosue Y, Shiina N, Tsukita S (2000). Adenomatous polyposis coli (APC) protein moves along microtubules and concentrates at their growing ends in epithelial cells. J Cell Biol 148, 505–518.
Mimori-Kiyosue Y, Tsukita S (2003). "Search-and-capture" of microtubules through plus-end-binding proteins (+TIPs). J Biochem 134, 321–326.
Miyashiro I, Senda T, Matsumine A, Baeg GH, Kuroda T, Shimano T, Miura S, Noda T, Kobayashi S, Monden M, *et al.* (1995). Subcellular localization of the APC protein: immunoelectron microscopic study of the association of the APC protein with catenin. Oncogene 11, 89–96.
Mogensen MM, Tucker JB, Mackie JB, Prescott AR, Nathke IS (2002). The adenomatous polyposis coli protein unambiguously localizes to microtubule plus ends and is involved in establishing parallel arrays of microtubule bundles in highly polarized epithelial cells. J Cell Biol 157, 1041–1048.
Morfini G, Szebenyi G, Brown H, Pant HC, Pigino G, DeBoer S, Beffert U, Brady ST (2004). A novel CDK5-dependent pathway for regulating GSK3 activity and kinesin-driven motility in neurons. EMBO J 23, 2235–2245.
Morrison EE (2009). The APC-EB1 interaction. Adv Exp Med Biol 656, 41–50.
Moser AR, Dove WF, Roth KA, Gordon JI (1992). The Min (multiple intestinal neoplasia) mutation: its effect on gut epithelial cell differentiation and interaction with a modifier system. J Cell Biol 116, 1517–1526.
Moser AR, Pitot HC, Dove WF (1990). A dominant mutation that predisposes to multiple intestinal neoplasia in the mouse. Science 247, 322–324.
Murphy JT, Tucker JM, Davis C, Berger FG (2004). Raltitrexed increases tumorigenesis as a single agent yet exhibits anti-tumor synergy with 5-fluorouracil in ApcMin/+ mice. Cancer Biol Ther 3, 1169–1176.
Musch A (2004). Microtubule organization and function in epithelial cells. Traffic 5, 1–9.
Nelson S, Nathke IS (2013). Interactions and functions of the adenomatous polyposis coli (APC) protein at a glance. J Cell Sci 126, 873–877.
Nieuwenhuis MH, Douma KF, Bleiker EM, Aaronson NK, Clevers H, Vasen HF (2012). Clinical evidence for an association between familial adenomatous polyposis and type II diabetes. Int J Cancer 131, 1488–1489.
Niho N, Takahashi M, Kitamura T, Shoji Y, Itoh M, Noda T, Sugimura T, Wakabayashi K (2003). Concomitant suppression of hyperlipidemia and intestinal polyp formation in Apc-deficient mice by peroxisome proliferator-activated receptor ligands. Cancer Res 63, 6090–6095.

Nirschl JJ, Magiera MM, Lazarus JE, Janke C, Holzbaur EL (2016). alpha-tubulin tyrosination and CLIP-170 phosphorylation regulate the initiation of dynein-driven transport in neurons. Cell Rep 14, 2637–2652.
Osawa E, Nakajima A, Wada K, Ishimine S, Fujisawa N, Kawamori T, Matsuhashi N, Kadowaki T, Ochiai M, Sekihara H, *et al*. (2003). Peroxisome proliferator-activated receptor gamma ligands suppress colon carcinogenesis induced by azoxymethane in mice. Gastroenterology 124, 361–367.
Park HK (2013). Metformin and cancer in type 2 diabetes. Diabetes Metab J 37, 113–116.
Pfalzer AC, Kamanu FK, Parnell LD, Tai AK, Liu Z, Mason JB, Crott JW (2016). Interactions between the colonic transcriptome, metabolome and microbiome in mouse models of obesity-induced intestinal cancer. Physiol Genomics 48, 545–553.
Pigino G, Morfini G, Pelsman A, Mattson MP, Brady ST, Busciglio J (2003). Alzheimer's presenilin 1 mutations impair kinesin-based axonal transport. J Neurosci 23, 4499–4508.
Raaijmakers JA, Tanenbaum ME, Medema RH (2013). Systematic dissection of dynein regulators in mitosis. J Cell Biol 201, 201–215.
Radulescu S, Ridgway RA, Appleton P, Kroboth K, Patel S, Woodgett J, Taylor S, Nathke IS, Sansom OJ (2010). Defining the role of APC in the mitotic spindle checkpoint in vivo: APC-deficient cells are resistant to Taxol. Oncogene 29, 6418–6427.
Ramjeesingh R, Orr C, Bricks CS, Hopman WM, Hammad N (2016). A retrospective study on the role of diabetes and metformin in colorectal cancer disease survival. Curr Oncol 23, e116–e122.
Reilein A, Nelson WJ (2005). APC is a component of an organizing template for cortical microtubule networks. Nat Cell Biol 7, 463–473.
Roberts AJ, Goodman BS, Reck-Peterson SL (2014). Reconstitution of dynein transport to the microtubule plus end by kinesin. eLife 3, e02641.
Ruane PT, Gumy LF, Bola B, Anderson B, Wozniak MJ, Hoogenraad CC, Allan VJ (2016). Tumour suppressor adenomatous polyposis coli (APC) localisation is regulated by both kinesin-1 and kinesin-2. Sci Rep 6, 27456.
Saltiel AR, Pessin JE (2002). Insulin signaling pathways in time and space. Trends Cell Biol 12, 65–71.
Sasazuki S, Charvat H, Hara A, Wakai K, Nagata C, Nakamura K, Tsuji I, Sugawara Y, Tamakoshi A, Matsuo K, *et al*. (2013). Diabetes mellitus and cancer risk: pooled analysis of eight cohort studies in Japan. Cancer Sci 104, 1499–1507.
Schneikert J, Brauburger K, Behrens J (2011). APC mutations in colorectal tumours from FAP patients are selected for CtBP-mediated oligomerization of truncated APC. Hum Mol Genet 20, 3554–3564.
Senda T, Miyashiro I, Matsumine A, Baeg GH, Monden T, Kobayashil S, Monden M, Toyoshima K, Akiyama T (1996). The tumor suppressor protein APC colocalizes with beta-catenin in the colon epithelial cells. Biochem Biophys Res Commun 223, 329–334.
Sharma M, Leung L, Brocardo M, Henderson J, Flegg C, Henderson BR (2006). Membrane localization of adenomatous polyposis coli protein at cellular protrusions: targeting sequences and regulation by beta-catenin. J Biol Chem 281, 17140–17149.
Steuer ER, Wordeman L, Schroer TA, Sheetz MP (1990). Localization of cytoplasmic dynein to mitotic spindles and kinetochores. Nature 345, 266–268.
Su LK, Kinzler KW, Vogelstein B, Preisinger AC, Moser AR, Luongo C, Gould KA, Dove WF (1992). Multiple intestinal neoplasia caused by a mutation in the murine homolog of the APC gene. Science 256, 668–670.
Tanneberger K, Pfister AS, Kriz V, Bryja V, Schambony A, Behrens J (2011). Structural and functional characterization of the Wnt inhibitor APC membrane recruitment 1 (Amer1). J Biol Chem 286, 19204–19214.
Thamotharan M, Bawani SZ, Zhou X, Adibi SA (1999). Hormonal regulation of oligopeptide transporter pept-1 in a human intestinal cell line. Am J Physiol 276, C821–C826.
Tontonoz P, Spiegelman BM (2008). Fat and beyond: the diverse biology of PPARgamma. Annu Rev Biochem 77, 289–312.
Vogtmann E, Hua X, Zeller G, Sunagawa S, Voigt AY, Hercog R, Goedert JJ, Shi J, Bork P, Sinha R (2016). Colorectal cancer and the human gut microbiome: reproducibility with whole-genome shotgun sequencing. PLoS One 11, e0155362.
Wang Y, Azuma Y, Friedman DB, Coffey RJ, Neufeld KL (2009). Novel association of APC with intermediate filaments identified using a new versatile APC antibody. BMC Cell Biol 10, 75.
Weaver C, Leidel C, Szpankowski L, Farley NM, Shubeita GT, Goldstein LS (2013). Endogenous GSK-3/shaggy regulates bidirectional axonal transport of the amyloid precursor protein. Traffic 14, 295–308.
Wen Y, Eng CH, Schmoranzer J, Cabrera-Poch N, Morris EJ, Chen M, Wallar BJ, Alberts AS, Gundersen GG (2004). EB1 and APC bind to mDia to stabilize microtubules downstream of Rho and promote cell migration. Nat Cell Biol 6, 820–830.
Whitehead RH, Joseph JL (1994). Derivation of conditionally immortalized cell lines containing the Min mutation from the normal colonic mucosa and other tissues of an "Immortomouse"/Min hybrid. Epithelial Cell Biol 3, 119–125.
Whitehead RH, VanEeden PE, Noble MD, Ataliotis P, Jat PS (1993). Establishment of conditionally immortalized epithelial cell lines from both colon and small intestine of adult H-2Kb-tsA58 transgenic mice. Proc Natl Acad Sci USA 90, 587–591.
Yan S, Zhang H, Hou G, Ahmed S, Williams JC, Polenova T (2015). Internal dynamics of dynactin CAP-Gly is regulated by microtubules and plus end tracking protein EB1. J Biol Chem 290, 1607–1622.
Yin S, Bai H, Jing D (2014). Insulin therapy and colorectal cancer risk among type 2 diabetes mellitus patients: a systemic review and meta-analysis. Diagn Pathol 9, 91.
Yuhara H, Steinmaus C, Cohen SE, Corley DA, Tei Y, Buffler PA (2011). Is diabetes mellitus an independent risk factor for colon cancer and rectal cancer. Am J Gastroenterol 106, 1911–1921; quiz 1922.
Zhou JY, Xu B, Li L (2015). A new role for an old drug: metformin targets microRNAs in treating diabetes and cancer. Drug Dev Res 76, 263–269.
Zumbrunn J, Kinoshita K, Hyman AA, Nathke IS (2001). Binding of the adenomatous polyposis coli protein to microtubules increases microtubule stability and is regulated by GSK3 beta phosphorylation. Curr Biol 11, 44–49.